

On the Magnetic Nature of Quantum Point Contacts

P. S. Cornaglia and C. A. Balseiro

*Instituto Balseiro and Centro Atómico Bariloche, Comisión Nacional de Energía Atómica,
8400 San Carlos de Bariloche, Río Negro, Argentina.*

We present results for a model that describes a quantum point contact. We show how electron-electron correlations, within the unrestricted Hartree-Fock approximation, generate a magnetic moment in the point contact. Having characterized the magnetic structure of the contact, we map the problem onto a simple one-channel model and calculate the temperature dependence of the conductance for different gate voltages. Our results are in good agreement with experimental results obtained in *GaAs* devices and support the idea of Kondo effect in these systems.

PACS numbers: 73.61.-r, 71.15.Mb, 71.70.Ej, 75.75.+a

Ballistic transport in quantum wires with ideal contacts leads naturally to conductance quantization in units of $2e^2/h$ [1, 2, 3]. This notable result has become one of the paradigms of mesoscopic physics. By a quantum wire we understand conductor that is so thin that the quantization of the transverse modes becomes important. In short quantum wires we have to expect also some quantization effects along the wire axis [4]. In some of these short wires and in quantum point contacts, as the gate voltage is varied, together with the $2e^2/h$ plateaus the conductance shows some structure at $0.7(2e^2/h)$ [5, 6, 7]. This structure has been systematically observed *GaAs* devices and is known as the 0.7 anomaly. Recent experiments presented evidence on the magnetic nature of this structure: for gate voltages at the 0.7 anomaly the conductance increases as the temperature is lowered, an effect that may be interpreted as a signature of Kondo effect [6]. The Kondo picture is supported by the scaling of the experimental data, that close to the 0.7 anomaly show a universal temperature dependence. Moreover the low temperature differential conductance presents a narrow structure at zero bias voltage, which splits with an in-plane magnetic field as due to a Kondo resonance. The conventional Kondo effect is the magnetic screening of a localized moment [8], if this effect is taking place in the quantum point contact (QPC), then the main question is: where and how is the magnetic moment generated? Recent spin dependent functional density calculations suggest the formation of a magnetic moment localized at the QPC for a device built on *GaAs* [9, 10, 11]. This scenario in which a magnetic moment is spontaneously generated by the electron-electron correlations is appealing since it naturally leads to the Kondo physics observed experimentally, however there are still many open questions related to the magnetic nature of the QPC and its relation to the 0.7 anomaly.

In this work we report results obtained for a model that describes a short QPC. We show how correlations, within the unrestricted Hartree-Fock approximation, induce a magnetic moment in the region of the constriction for some values of the gate voltages. Having characterized the magnetic properties of the QPC, we map the problem

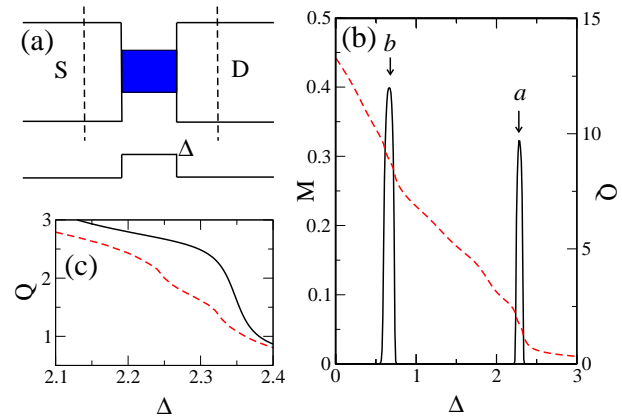


FIG. 1: (a) Schematic picture of the model for the QPC, the potential at the constriction is Δ . (b) Magnetic moment (continuous line) and total charge (dashed line) at the constriction of a 3-site-wide and 9-site-long QPC. The first conduction channel opens at a and the second at b , the large magnetization at these points signals the formation of a local magnetic moment. The local interaction is $U = 2.0$ and the Fermi energy is $\epsilon_F = -0.95$, with all parameters in units of $t = 1$. The source and drain slabs have a width of 10 sites. (c) Detail of the total charge around a (dashed line) compared with a non-interacting system (continuous line).

onto a simple one-channel model, then using the numerical renormalization group we calculate the conductance for different gate voltages and temperatures. Our results are in agreement with the experimental observations and support the idea of a Kondo effect in these systems.

For the sake of simplicity we resort to a one band Hubbard model with local interactions.

$$H = \sum_{i,\sigma} \epsilon_i c_{i\sigma}^\dagger c_{i\sigma} + U \sum_i c_{i\uparrow}^\dagger c_{i\uparrow} c_{i\downarrow}^\dagger c_{i\downarrow} - t \sum_{i,j,\sigma} c_{j\sigma}^\dagger c_{i\sigma} \quad (1)$$

here $c_{i\sigma}$ annihilates an electron with spin σ at site i , U is the on-site Coulomb repulsion and the last term in Eq. (1) describes the nearest neighbor hopping with matrix element t . The on-site energy ϵ_i describes the potential at the QPC. For simplicity, in what follows we use a square potential parametrized with a single variable Δ : using the geometry of Fig. 1(a) we take $\epsilon_i = 0$

for i in the source and drain, and $\varepsilon_i = \Delta, \infty$ for i in the contact and at the sides of the contact respectively. The energy Δ can be controlled by a gate potential V_g and we may consider $\Delta \propto -|e|V_g$. The square potential maximizes resonances for states with wavelengths commensurate with the point contact, nevertheless smoother potentials with more parameters give similar results. Below we comment on the details that are sensitive to the shape of the QPC. We look for the ground state of Hamiltonian (1) in the unrestricted Hartree-Fock approximation for slabs with a QPC as in Fig. 1(a). In the central region [between dashed lines in Fig. 1(a)], the expectation value of the electron number for each spin and at each site is calculated self-consistently. Away from the constriction, in the source and drain, we use the Hartree-Fock solution of a uniform system with approximately 0.5 electrons per site. For the results presented below, we checked that the boundary between the two regions is far enough from the contact so that the solution becomes independent of its position. Given the geometry, i.e., the length and the width of the point contact, and the value of U within a wide interval, we find that for some values of the gate voltage V_g a magnetic moment is formed in the region of the constriction. We define the total charge Q and the magnetization M of the contact as the expectation value of the operators $\hat{O} = \sum'_{i,\sigma} c_{i\sigma}^\dagger c_{i\sigma}$ and $\hat{M} = \frac{1}{2} \sum'_i (c_{i\uparrow}^\dagger c_{i\uparrow} - c_{i\downarrow}^\dagger c_{i\downarrow})$ where the sum is over all the sites of the QPC. The results are summarized in Fig. 1(b): for large negative gate voltages the total charge Q in the point contact is exponentially small. As Δ decreases (V_g increases) Q increases and for some values of the gate potential there is an abrupt increase in the total charge. At the step-like structures obtained around the point marked as a in Fig. 1(b) [see also detail in 1(c)], approximately one electron is transferred from the source and drain to the point contact. This behavior in Q is characteristic of Coulomb blockade. Between the two first steps in Q there is a spin 1/2 localized at the point contact as indicated by the magnetization curve shown also in Fig. 1(b). At the point a of Fig. 1(b), where a spin 1/2 local moment is stable, a narrow resonance is crossing the Fermi energy. This resonance is clearly seen in the local density of states (LDOS) of the QPC as shown in Fig. 2(a). This first resonance corresponds to a state with no nodes in the QPC as can be inferred from the magnetization of Fig. 2(c). Note that the magnetic moment is localized at the QPC. At the point marked as b in Fig. 1(b) again a spin 1/2 is localized in the QPC, this is due to a resonance of the second channel crossing the Fermi energy. That this magnetic moment is due to a resonance of the second channel can be inferred by the magnetization profile that has a node along the major axis of the QPC as shown in Fig. 2(d). When the chemical potential coincides with a narrow resonance, the system Hamiltonian can be mapped into that of an An-

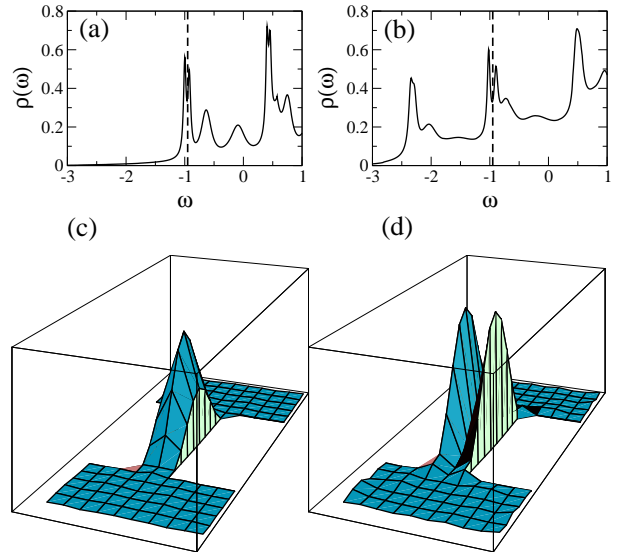


FIG. 2: (a) Average in the QPC region of the total local density of states (spin up plus spin down) for the system of Fig. 1(b) and $\Delta = 2.27$. (b) Same as (a) with $\Delta = 0.66$. The vertical dashed line in (a) and (b) marks the position of the Fermi level. (c) and (d) spatial distribution of the magnetization for the (a) and (b) situations respectively.

derson impurity [12] with effective interaction U_{eff} and resonance width Γ_{eff} . If $U_{eff} \gtrsim \pi\Gamma_{eff}$, in analogy with Anderson criterion for magnetic impurities [8], we expect a magnetic moment in the QPC. The effective parameters scale with the size of the QPC as: $U_{eff} \sim U/A$ where A is the area of the QPC and, for the geometry of Fig. 1(a), $\Gamma_{eff} \propto 1/L^3$, where L is the length of the QPC [13].

These results deserve a few comments:

i.- The behavior of Q as function of Δ and the occurrence of a local magnetic moment in the QPC is reproduced for a wide range of values of the Coulomb repulsion U . For the electron densities used up to now (~ 0.5 electrons per site), the critical value of U that generates a global instability U_c is larger than $8t$. The behavior presented in Fig. 1(b) corresponds to $U = 2t$, far away from the global instability, and is qualitatively reproduced for wide range of U values.

ii.- The formation of a local magnetic moment is not a peculiarity of the model used to simulate the potential due to the gate voltage. We have analyzed different potentials to show that the local instabilities shown in Fig. 1(b), are robust for potentials that have a flat region and produce resonances. Conversely, for wedge-like point contacts [1], the Hartree-Fock solution does not show a magnetic moment for moderate values of U .

iii.- For the geometries of Fig. 1(a), narrow resonances are obtained at the bottom of each channel band. Localized magnetic moments are then obtained each time a new channel becomes active in agreement with Ref. 7. The details of the magnitude and spatial distribution of

the magnetic moment depend on the shape of the QPC potential.

iv.- The Hartree-Fock approximation, as well as other methods like the spin dependent functional density approximation [11], can not be fully satisfactory since they break the local symmetry. In the exact solution of the problem, spin fluctuations should recover local rotational invariance. However as for the original problem of magnetic moment formation in impurities [8], the Hartree-Fock results do indicate the region in parameter space where we can expect magnetic fluctuations to play a central role in the low energy physics. A detailed analysis of the local Hartree-Fock instability for different parameters and QPC shapes will be presented elsewhere [13].

To go beyond the Hartree-Fock approximation and to make a connection with the Kondo problem a simplification of the model is required. To do so, we first revisit the transport properties of a non-interacting QPC. Using the Keldysh formalism and the zero temperature Landauer expression, the conductance of an infinite slab with a constriction as the one described above [Fig. 1(a)] is given by [3, 14]

$$G = \frac{e^2}{h} \text{Tr} [\Gamma_L \mathbf{G}^R \Gamma_R \mathbf{G}^A] \Big|_{\omega=\varepsilon_F} \quad (2)$$

where $\mathbf{G}^{R(A)}$ are matricial retarded (advanced) Green functions with elements $[\mathbf{G}^{R(A)}]_{i,j}$ where i and j indicate two sites of the neck of the QPC, the matrices Γ_l where l indicates right and left describe the coupling to the leads and are given by

$$\Gamma_l = i [\Sigma_l^R - \Sigma_l^A]$$

where $\Sigma_l^{R(A)}$ are the self energies due to the leads. The conductance as a function of the gate voltage V_g is shown in Fig. 3(a). Again the details depend on the potential used to describe the QPC, with the square potential the maximums reach the conductance quantum $2e^2/h$ while with smoother potentials the amplitude of the oscillations decreases and the maximums do not necessarily reach the conductance quantum. The results presented in the figure are characteristic of potentials having a flat region along the major QPC axis, even if the potential smoothly decreases toward its source and drain value. The conductance for longer QPC oscillates more rapidly since resonances are narrower and closer in energy. We note that here, when the conductance in units of $2e^2/h$ is smaller than one, the transmission is due to a single channel. In this one channel regime, and at low enough temperatures, we can map the problem onto an effective one-dimensional (1D) model. In what follows we present a model that, in the gate voltage interval indicated with vertical dashed lines in Fig. 3(a), reproduces the structure of the conductance and of the density of states. In Fig. 3(b) a schematic picture of a linear chain with a 3-site central region representing the QPC is shown. To reproduce the structure we adjust the hybridization of the

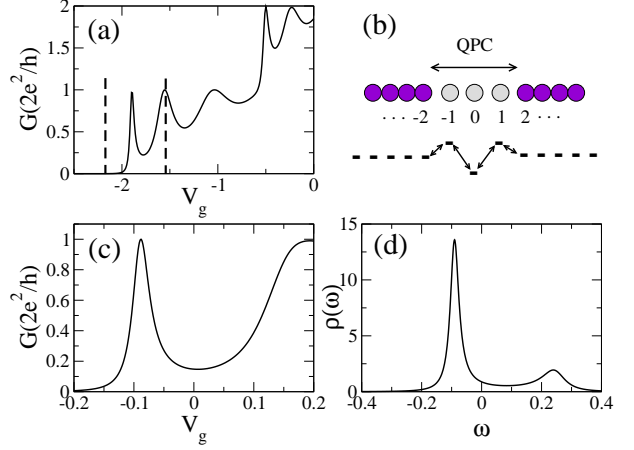


FIG. 3: (a) Conductance for a 3×9 QPC in a non-interacting system as a function of the barrier height in the QPC region. (b) Effective 1D model to describe the first step in (a). (c) Conductance and (d) local density of states at the central site of (b) for a QPC with $\epsilon_0 = -V_g$, $\epsilon_1 = \epsilon_{-1} = -V_g + 0.15$, $V = 0.15/\sqrt{2}$, and $t_{1,2} = t_{-1,-2} = 0.25$.

central site V , those of the adjacent sites $t_{1,2} = t_{-1,-2}$ and the diagonal energies ϵ_0 and $\epsilon_{-1} = \epsilon_1$. The diagonal energies are all shifted linearly with V_g . The conductance as a function of a gate voltage for this 1D model, shown in Fig. 3(c), reproduces the first structures of Fig. 3(a). The first peak in the conductance is due to a resonant state crossing the Fermi level. This resonance is observed in the local density of states (LDOS) of the central site as shown in Fig. 3(d). Having this non-interacting 1D model that mimics the transport properties of the QPC, we can now turn on the interaction that generates a local moment. The local moment should be associated with the first resonance in the LDOS and then we include a local interaction at the central site. The temperature dependence of the conductance for this model in the linear regime can be calculated exactly using the numerical renormalization group [15]. We proceed as in Ref. 16 to put the conductance in terms of the spectral density of the correlated site $\rho_0(\omega)$.

$$G(T) = \frac{2e^2}{h} 2\pi \int d\omega \left(-\frac{\partial f(\omega)}{\partial \omega} \right) \Gamma(\omega) \rho_0(\omega) \quad (3)$$

where $f(\omega)$ is the Fermi function, and $\Gamma(\omega) = \pi V^2 \rho_1(\omega)$ with $\rho_1(\omega)$ the spectral density of site 1 with $V = 0$.

The results are shown in Fig. 4(a) and 4(b), for two sets of parameters, where the conductance is plotted as function of the gate voltage for different temperatures. The numerical results are notably similar to the experiments of Ref. 6. At intermediate temperatures the conductance presents a plateau at about $0.7(2e^2/h)$. This structure is not universal, depending on the parameters a more pronounced maximum can be obtained and the whole structure can be slightly shifted up or down. As the temper-

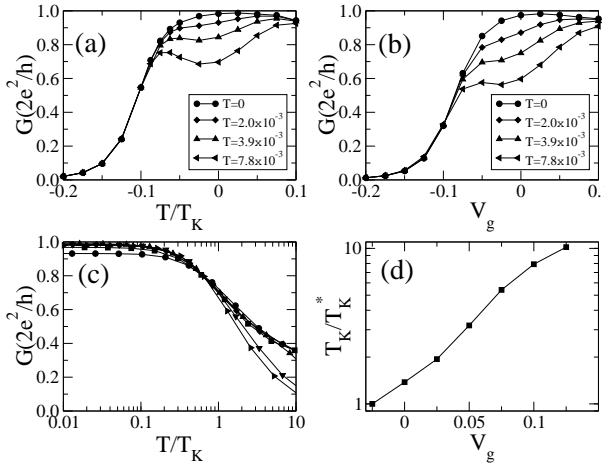


FIG. 4: (a) Conductance as a function of the gate voltage V_g for the one-dimensional model of Fig. 2(b) with $U = 1.0$ in the central site and the other parameters as in Fig. 2(c). (b) Same as (a) with $V = 0.2/\sqrt{2}$ and $\epsilon_1 = \epsilon_{-1} = -V_g + 0.25$. (c) Conductance as a function of the scaled temperature for the parameters in (a). (d) Kondo temperature obtained from the scaling in (c), $T_K^* = T_K(V_g = -0.05) = 1.5 \times 10^{-3}$.

ature decreases the conductance increases toward $2e^2/h$. The conductance as a function of temperature for different values of the gate voltage is shown in Fig. 4(c). At low temperatures, all the curves collapse into a single one when the temperature is properly scaled. We define the Kondo temperature T_K as the scaling parameter. Contrary to what is obtained in the conventional Anderson model [8], in our mapping the Kondo temperature increases as the gate voltage increases and the resonance is pushed *away* from the Fermi level. This is in agreement with the experimental observation and is due to an increase of the density of states at the Fermi energy as V_g increases and the second longitudinal resonance approaches the Fermi level.

In summary we have studied the formation of a magnetic moment in quantum point contacts and its relation with the observed anomalies in transport experiments. On the one hand the Hartree-Fock picture presented here accounts for the occurrence magnetic moments when resonant states of the QPC are aligned with the Fermi level. For a moderate local interaction, the stable local magnetic moments are related only to the first longitudinal resonance of each transverse mode, i.e., at the beginning of each conductance step, in agreement with the results of Reilly *et al.* [7]. However, the behavior of the conductance at each conductance step will depend of the particular details of the QPC potential. These results are robust for QPC that generate a flat potential along the contact axis. Wedge-like contacts do not generate sharp resonances and consequently no strong magnetic fluctua-

tion develop at the contact region. However the conductance could show some structure depending on the electronic structure in the QPC region. On the other hand, by mapping the problem onto a one-channel model, we calculated the temperature and gate voltage dependence of the conductance that are in good agreement with the experimental observation. Our results support the idea of Kondo effect in the point contact however our proposal differs from previous ones: in the work by Meir *et al.* [11] it is assumed that as the gate voltage is increased, the magnetic moment is formed well before the conductance increases although it is essentially decoupled from the electron gas. In our approach the conductance increase is accompanied by the formation of the magnetic moment and this occurs each time a new channel starts to participate in the transport through the point contact. Our one-channel numerical renormalization group results are essentially exact and can describe different situations with the same precision including the situation at which the magnetic moment is being formed as well as the Kondo regime.

Acknowledgment: We thank B. Alascio for stimulating discussions. This work was partially supported by the CONICET and ANPCYT, grants N. 02151 and 99 3-6343

- [1] B.J. van Wees, *et al.*, Phys. Rev. Lett. **60**, 848 (1988).
- [2] D.A. Wharam, *et al.*, J. Phys. C **21**, L209 (1988).
- [3] S. Datta, *Electronic Transport in Mesoscopic Systems* (Cambridge University, Cambridge, England, 1995).
- [4] D.J. Reilly, *et al.*, Phys. Rev. B **63**, R121311 (2001).
- [5] K.J. Thomas, *et al.*, Phys. Rev. Lett. **77**, 135 (1996); K.J. Thomas, *et al.*, Phys. Rev. B **58**, 4846 (1998).
- [6] S.M. Cronenwett, *et al.*, Phys. Rev. Lett. **88**, 226805 (2002).
- [7] D.J. Reilly, *et al.*, Phys. Rev. Lett. **89**, 246801 (2002).
- [8] For a review, see A.C. Hewson, *The Kondo problem to heavy fermions* (Cambridge University, Cambridge, England, 1993).
- [9] K.-F. Berggren and I. I. Yakimenko, Phys. Rev. B **66**, 085323 (2002).
- [10] K. Hirose, Y. Meir, and N.S. Wingreen, Phys. Rev. Lett. **90** 026804 (2003).
- [11] Y. Meir, K. Hirose, and N.S. Wingreen, Phys. Rev. Lett. **89** 196802 (2002).
- [12] P.W. Anderson, Phys. Rev. **124**, 41 (1961).
- [13] P.S. Cornaglia, M. Avignon, and C.A. Balseiro, (unpublished).
- [14] H.M. Pastawski, Phys. Rev. B **44**, 6329 (1991); *ibid.* **46**, 4053 (1992).
- [15] K.G. Wilson, Rev. Mod. Phys. **47**, 773 (1975); H.R. Krishna-murthy, J.W. Wilkins, and K.G. Wilson Phys. Rev. B **21**, 1044 (1980).
- [16] P.S. Cornaglia and C.A. Balseiro, cond-mat/0212119.